Separation Science and Technology
Publication details, including instructions for authors and subscription information:
http://www.informaworld.com/smpp/title~content=t713708471

Adsorption of *o*-Cresol and Benzoic Acid in an Adsorber Packed with an Ion-Exchange Resin: A Comparative Study of Diffusional Models

Run-Tun Huang[a]; Teh-Liang Chen[a]; Hung-Shan Weng[a]
[a] DEPARTMENT OF CHEMICAL ENGINEERING, NATIONAL CHENG KUNG UNIVERSITYTAINAN, TAINAN, TAIWAN, REPUBLIC OF CHINA

To cite this Article Huang, Run-Tun , Chen, Teh-Liang and Weng, Hung-Shan(1994) 'Adsorption of *o*-Cresol and Benzoic Acid in an Adsorber Packed with an Ion-Exchange Resin: A Comparative Study of Diffusional Models', Separation Science and Technology, 29: 15, 2019 — 2033
To link to this Article: DOI: 10.1080/01496399408002187
URL: http://dx.doi.org/10.1080/01496399408002187

SEPARATION SCIENCE AND TECHNOLOGY, 29(15), pp. 2019–2033, 1994

Adsorption of *o*-Cresol and Benzoic Acid in an Adsorber Packed with an Ion-Exchange Resin: A Comparative Study of Diffusional Models

RUN-TUN HUANG, TEH-LIANG CHEN, and
HUNG-SHAN WENG*
DEPARTMENT OF CHEMICAL ENGINEERING
NATIONAL CHENG KUNG UNIVERSITY
TAINAN, TAIWAN 70101, REPUBLIC OF CHINA

ABSTRACT

Both solid- and pore-diffusion models were employed to simulate the adsorption of *o*-cresol and benzoic acid in a fixed-bed adsorber packed with an anion-exchange resin. The equilibrium adsorption data were modeled by a Langmuir isotherm. When the shape of the adsorption isotherm was approximately linear (as in the case of *o*-cresol), both models agreed well with the experimental breakthrough data, and they could be effectively applied to predict the breakthrough curve of longer columns. For a favorable adsorption isotherm (say, benzoic acid), however, better results were obtained by using the solid-diffusion model. In addition to the shape of the adsorption isotherm, several factors, such as the type of adsorbent, modeling of equilibrium data, computation efficiency, and concentration dependence of the intraparticle diffusivity, should also be taken into account for selecting a suitable diffusion model.

Key Words. Fixed-bed adsorber; Breakthrough curve; Diffusion model; Ion-exchange resin

INTRODUCTION

Prediction of breakthrough curves is the goal of most theoretical treatments for a fixed-bed adsorption column. In modeling the system, both solid- and pore-diffusion models have been widely used (1–5). The basic

* To whom correspondence should be addressed.

difference in these two models is the description of the diffusional process within the adsorbents. In the solid-diffusion model, the adsorption process is assumed to occur at the outer surface of the adsorbents, followed by the diffusion of the adsorbate in the adsorbed state. The pore-diffusion model, on the other hand, assumes a distributed adsorption along the pore walls during diffusion of a fluid into the pore of the adsorbents. The effect of the diffusion model on simulating a breakthrough curve has been previously reported in the work of Weber and Chakravorti (2). They indicated that the choice of the two models for an adsorption bed is not important if the adsorption isotherm is linear, while care should be exercised in selecting a diffusion model for cases of nonlinear isotherms. However, the shape of adsorption isotherm is not the only factor that should be considered in selecting a diffusion model, and the effect of diffusion model on the simulation needs still greater attention. The motivation for this study comes from the scarcity of information concerned with the suitability of employing a diffusion model to simulate a fixed-bed adsorption column.

The adsorption isotherms of *o*-cresol and benzoic acid on an anion-exchange resin differ greatly. Equilibrium data showed an approximately linear adsorption isotherm for *o*-cresol and a favorable one for benzoic acid, as given in Figs. 1 and 2. Accordingly, they form a good comparative

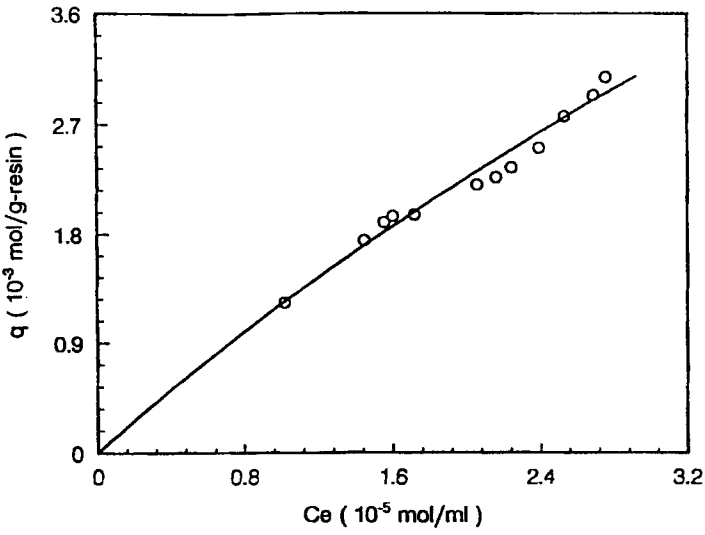

FIG. 1 Equilibrium isotherm of *o*-cresol at 27°C. Open circles, experimental data; solid line, Langmuir isotherm based on $C_0 = 2.778 \times 10^{-5}$ mol/mL and $\alpha = 1.253$.

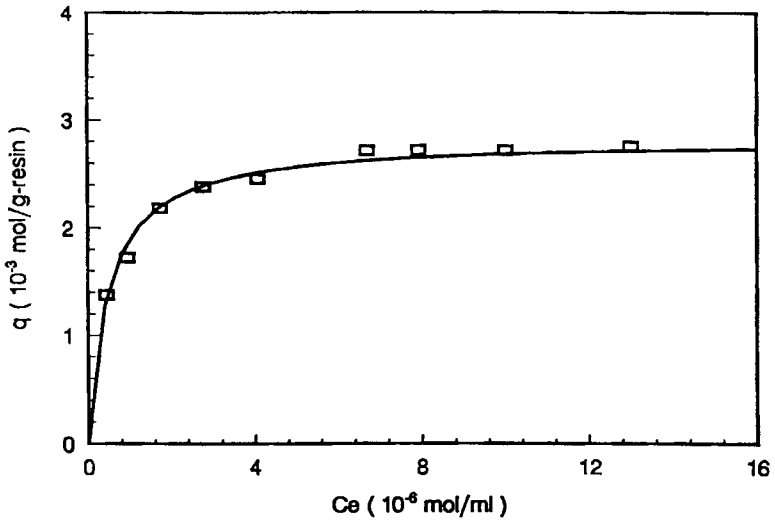

FIG. 2 Equilibrium isotherm of benzoic acid at 27°C. Open squares, experimental data; solid line, Langmuir isotherm based on $C_0 = 1.639 \times 10^{-5}$ mol/mL and $\alpha = 34.32$.

basis for assessing various diffusional models for prediction of breakthrough curves. In the present work, the suitability of both solid- and pore-diffusion models for the adsorption of *o*-cresol and benzoic acid on a fixed-bed column was examined in the following ways. First, experiments were performed to obtain the breakthrough data for each of the two adsorbates. Second, the parameters unobtainable in both models were estimated by fitting the models to the experimental breakthrough data. Third, adsorptions were carried out on longer columns, with all other operational variables kept unchanged if at all possible. Fourth, the predicted breakthrough curves for the new adsorption beds, generated from both models with the corresponding estimated parameters, were compared with the experimentals.

MATHEMATICAL MODELS

Modeling a fixed-bed adsorption column requires three essential equations. One is the mobile phase mass balance, describing the concentration of adsorbate in the bed void as the fluid passes through. The second equation is the intraparticle mass balance, describing the diffusion process within the pellets. The third equation describes the external film diffusion, which is the link between the first two equations. In the following two

models, the adsorption rate is assumed to be much faster than the diffusion rate, so that equilibrium exists at every local position.

Solid-Diffusion Model

The mass transfer processes describing the fixed-bed adsorber, packed with spherical particles of radius R, are assumed to include axial dispersion, particle diffusion, external film diffusion, and a Langmuir-type adsorption isotherm. The breakthrough curve can thus be obtained from the following set of equations.

Mobile phase mass balance:

$$\frac{\partial C}{\partial t} + v\frac{\partial C}{\partial z} - D_L\frac{\partial^2 C}{\partial z^2} = -\frac{1-\epsilon_b}{\epsilon_b}\rho D_s\left(\frac{3}{R}\right)\frac{\partial q}{\partial r}\bigg|_{r=R} \tag{1}$$

Particle diffusion:

$$\frac{\partial q}{\partial t} = D_s\left(\frac{\partial^2 q}{\partial r^2} + \frac{2}{r}\frac{\partial q}{\partial r}\right) \tag{2}$$

External film diffusion:

$$\rho D_s\frac{\partial q}{\partial r} = k_f(C - C_s), \qquad \text{at } r = R \tag{3}$$

Langmuir adsorption isotherm (6):

$$\frac{q}{q_0} = \frac{\alpha C_s/C_0}{1 + (\alpha - 1)C_s/C_0} \tag{4}$$

Initial conditions:

$$C = 0, \qquad \text{at } t = 0 \tag{5}$$

$$q = 0, \qquad \text{at } t = 0 \tag{6}$$

Boundary conditions:

$$C = C_0, \qquad \text{at } z = 0 \tag{7}$$

$$\partial C/\partial z = 0, \qquad \text{at } z = L \tag{8}$$

$$\partial q/\partial r = 0, \qquad \text{at } r = 0 \tag{9}$$

It should be noted that, in Eq. (4), q_0 is the solid phase concentration of the solute in equilibrium with the inlet concentration C_0 of the solute. By this expression, the Langmuir coefficient α is not a constant; instead, it varies with the inlet concentration C_0, as illustrated later.

Pore-Diffusion Model

This model pictures the adsorbate diffusing in the pores of the adsorbent and being adsorbed on the interior surface. Again, the mass transfer processes are assumed to include axial dispersion, intraparticle diffusion, external film diffusion, and a Langmuir isotherm.

Mobile phase mass balance:

$$\frac{\partial C}{\partial t} + v\frac{\partial C}{\partial z} - D_L\frac{\partial^2 C}{\partial z^2} = -\frac{1-\epsilon_b}{\epsilon_b}D_e\left(\frac{3}{R}\right)\frac{\partial C_p}{\partial r}\bigg|_{r=R} \tag{10}$$

Intraparticle mass balance:

$$\epsilon_p\frac{\partial C_p}{\partial t} + \rho\frac{\partial q}{\partial t} = D_e\left(\frac{\partial^2 C_p}{\partial r^2} + \frac{2}{r}\frac{\partial C_p}{\partial r}\right) \tag{11}$$

External film diffusion:

$$D_e\frac{\partial C_p}{\partial r} = k_f(C - C_p), \qquad \text{at } r = R \tag{12}$$

Langmuir adsorption isotherm:

$$\frac{q}{q_0} = \frac{\alpha C_p/C_0}{1 + (\alpha - 1)C_p/C_0} \tag{13}$$

Initial conditions:

$$C = 0, \qquad \text{at } t = 0 \tag{14}$$

$$C_p = 0, \qquad \text{at } t = 0 \tag{15}$$

$$q = 0, \qquad \text{at } t = 0 \tag{16}$$

Boundary conditions:

$$C = C_0, \qquad \text{at } z = 0 \tag{17}$$

$$\partial C/\partial z = 0, \qquad \text{at } z = L \tag{18}$$

$$\partial C_p/\partial r = 0, \qquad \text{at } r = 0 \tag{19}$$

MATERIALS AND METHODS

The adsorbent used for this study was Ion Exchanger II (weak base, Merck, Art No. 4766). The particles were sieved to 28–35 mesh. To convert the resin to OH-form, the resin was immersed in 1 N NaOH solution,

and then filtrated, washed with distilled water, and dried at room temperature for a couple of days. The average diameter of the swollen resin, measured by a profile projector, was 0.02522 cm. The apparent density of the wet resin was found to be 0.476 g/mL, and its true density was 1.116 g/mL. The moisture content, obtained from the difference of the weights of the swollen resin (centrifuging at 3,000 rpm for 5 minutes) and the dried resin (vacuum drying at 50°C for 8 hours), was 0.450. The void fraction of the resin thus calculated was 0.455.

Adsorption equilibria for *o*-cresol and benzoic acid were obtained by immersing various amounts of the resin in 50 mL of 4 g/L *o*-cresol solution and 2 g/L benzoic acid solution, respectively. The concentrations of the solute are represented by C_i in Eq. (20). Equilibrium was achieved in a shaker for about 6 days at 27°C. After equilibrium, the concentrations of *o*-cresol and benzoic acid (i.e., C_e in Eq. 20) were determined by a UV spectrophotometer (Hitachi, Model U-2000) at wavelengths of 275 and 268 nm, respectively. The amount of the solute adsorbed on the resin q was obtained by mass balance, i.e.,

$$q = \frac{(C_i - C_e)V}{W} \tag{20}$$

The column used for breakthrough measurements was a glass tube of 1.142 cm i.d. The solutions were fed upward in all the experiments. The void fraction in the bed, ϵ_b, was estimated from the volume of water which occupied the intergranule space in the ion-exchange column. Thus, ϵ_b was calculated from

$$\epsilon_b = 1.05 \times \frac{\text{volume of drained water}}{\text{bed volume}} \tag{21}$$

where 1.05 was used to account for the inclusion of incomplete drainage of water from the bed (7). The values of the bed void fraction obtained in all experiments were around 0.35.

The axial dispersion coefficient for the liquid flowing through fixed beds was obtained from the following correlation equation (8):

$$\frac{D_L \rho_L}{\mu} = \frac{\text{Re}}{0.20 + 0.011\text{Re}^{0.48}} \tag{22}$$

Equation (22) is applicable in the Reynolds number range of 10^{-3} to 10^3.

The film mass transfer coefficient k_f was calculated from (9, 10)

$$\frac{2Rk_f}{D_m} = 2.0 + 1.45\text{Re}^{1/2}\text{Sc}^{1/3} \tag{23}$$

where the molecular diffusivity, D_m, was estimated from the equation of Wilke and Chang (11).

To obtain the breakthrough curves generated from the two models, the dimensionless forms of Eqs. (1)–(9) and (10)–(19) were first treated by the orthogonal collocation method. The resulting ordinary differential equations were then solved by the method of DGEAR. The number of collocation points used varied from 5 to 8 for both column length and particle radius. Intraparticle diffusivity (D_s or D_e) was determined by fitting the model breakthrough curve to that of the experiment, in which the method of modified Fibonacci search (or golden section search) (12) was employed for the one-dimensional parameter estimation. The optimization criterion chosen was the minimum total square error. All the computations were done on a 486 personal computer.

RESULTS AND DISCUSSION

Conventionally, the Langmuir adsorption isotherm is expressed as

$$\frac{q}{q_m} = \frac{KC}{1 + KC} \tag{24}$$

where K is a constant and q_m is the maximum capacity of adsorption. q_m can be represented as the amount of adsorption at very high solute concentration. However, q_m is difficult to determine due to the following reasons. First, at very high liquid-phase concentrations, the amount of adsorption onto the solid phase is comparatively very small. The result is that the decrease in the liquid-phase solute concentration cannot be precisely measured. Second, high-concentration solutions may not be feasible due to the limitation of solubility. Third, the structure of the ion-exchange resin, and thus q_m, may be varied after adsorbing large amounts of solute. Fortunately, knowing the value of q_m is not necessary. Recall that q_0 is the solid-phase concentration of solute in equilibrium with the inlet concentration C_0. According to Eq. (24), we have

$$\frac{q_0}{q_m} = \frac{KC_0}{1 + KC_0} \tag{25}$$

Dividing Eq. (24) by Eq. (25), q_m can be dropped:

$$\frac{q}{q_0} = \frac{(1 + KC_0)C/C_0}{1 + [(1 + KC_0) - 1]C/C_0} = \frac{\alpha C/C_0}{1 + (\alpha - 1)C/C_0} \tag{26}$$

where $\alpha = 1 + KC_0$. Thus, a plot of α as a function of C_0 will give a straight

line of slope K and a vertical-axis intercept of 1. Once K is obtained, q_m can be calculated easily from Eq. (25) with the equilibrium data of C_0 versus q_0.

The data of adsorption equilibrium of *o*-cresol and benzoic acid on Ion Exchanger II are given in Figs. 1 and 2, respectively. The adsorption of *o*-cresol on the resin is roughly a linear isotherm, while benzoic acid yields a nonlinear (favorable) isotherm; nevertheless, both can be modeled by the Langmuir isotherm. The Langmuir coefficient α obtained was 1.253 for *o*-cresol based on a C_0 of 2.778×10^{-5} mol/mL, and 34.32 for benzoic acid if C_0 was taken as 1.639×10^{-5} mol/mL.

The experimental breakthrough data for *o*-cresol on a column of 10 cm length is shown in Fig. 3. The operational variables measured (or calculated) were: $C_0 = 2.778 \times 10^{-5}$ mol/mL, $\epsilon_b = 0.345$, $v = 17.64$ cm/min, $D_L = 1.474$ cm^2/min, and $k_f = 0.1479$ cm/min. In the solid-diffusion model, the only parameter remaining unavailable was D_s. Its value was estimated to be 1.634×10^{-7} cm^2/min by means of the one-parameter search process described above. The agreement of the calculated breakthrough curve to that of experiment is quite good (see 10-cm line). The estimated D_s was then used to predict breakthrough curves for longer adsorption beds, namely, 20 and 30 cm in length. Since the bed void fraction ϵ_b varied slightly in the new column runs, the interstitial fluid velocities v were remeasured as 17.25 and 17.40 cm/min, respectively. As

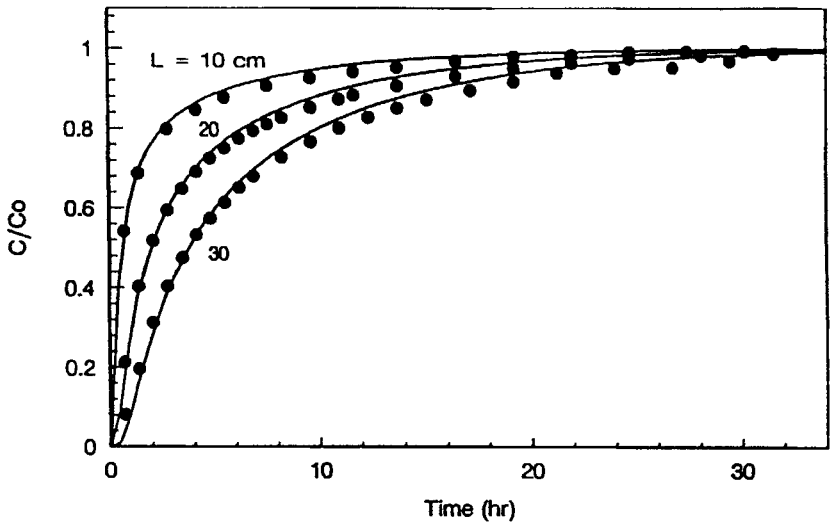

FIG. 3 Breakthrough curves for *o*-cresol with the solid diffusion model. Solid circles, experimental data; solid lines, fitting (10 cm) and prediction (20 and 30 cm).

Fig. 3 indicates (see 20- and 30-cm lines), the predicted breakthrough curve coincides with the experimental data. With the same sets of breakthrough data, the simulation was again performed based on the pore-diffusion model, and the results are shown in Fig. 4. Instead of D_s, the parameter estimated here was D_e. Its value was obtained as 1.875×10^{-5} cm²/min. As can be seen in Fig. 4, fitting of the model breakthrough curve to that of experiment is also excellent (see 10-cm line), and the results of prediction are quite satisfactory (see 20- and 30-cm lines). Therefore, it is suggested that the choice of diffusion model is not significant for roughly linear adsorption isotherms.

The same analysis was carried out for benzoic acid, and the results are shown in Figs. 5 and 6. For the experiment on a 10-cm column, the operational variables employed were: $C_0 = 1.639 \times 10^{-5}$ mol/mL, $\epsilon_b = 0.345$, $v = 18.20$ cm/min, $D_L = 1.519$ cm²/min, and $k_f = 0.1476$ cm/min. The intraparticle diffusivities for both solid- and pore-diffusion models, D_s and D_e, were estimated to be 1.258×10^{-7} and 1.626×10^{-5} cm²/min, respectively. It can be seen from Figs. 5 and 6 that both models can fit the experiment quite well (shown on the 10-cm lines). As for the prediction of 20- and 30-cm columns, the model breakthrough curves generated from the solid model have excellent coincidence with the experimental data, while they reach the saturation point (i.e., $C/C_0 = 1$) slightly

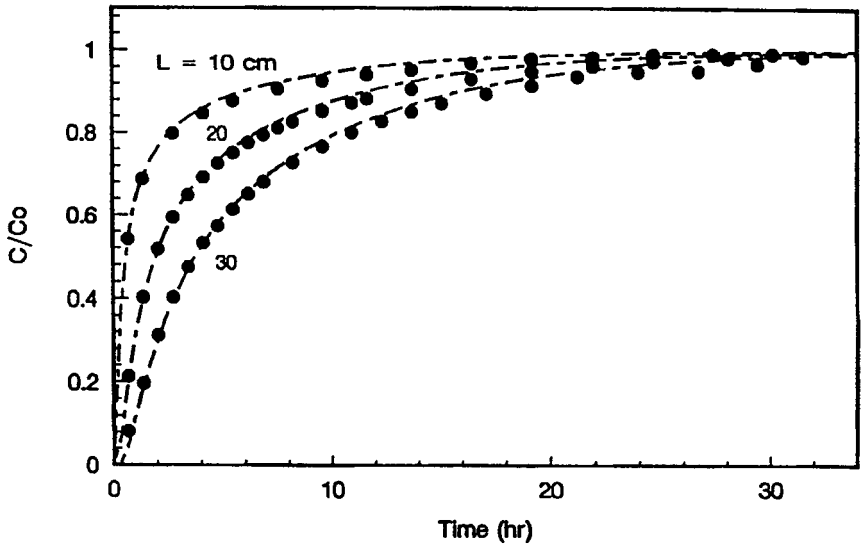

FIG. 4 Breakthrough curves for *o*-cresol with the pore diffusion model. Solid circles, experimental data; dashed lines, fitting (10 cm) and prediction (20 and 30 cm).

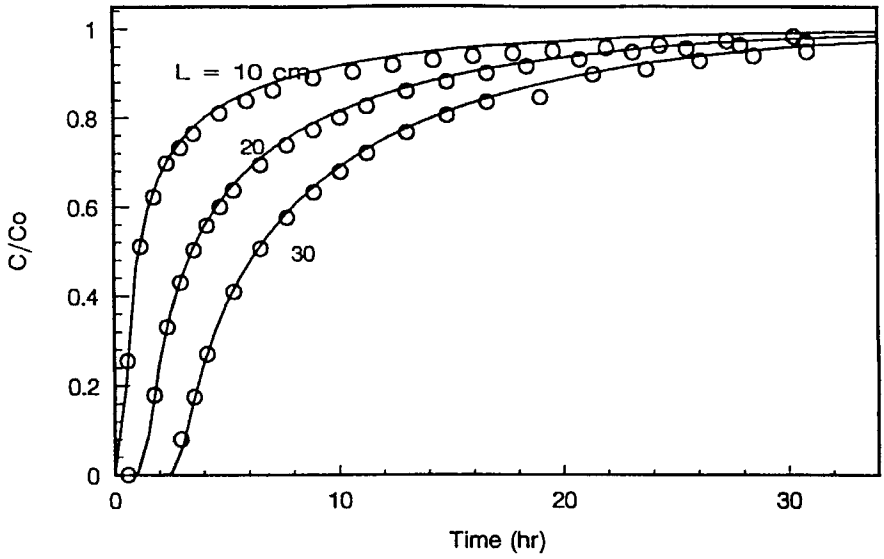

FIG. 5 Breakthrough curves for benzoic acid with the solid diffusion model. Open circles, experimental data; solid lines, fitting (10 cm) and prediction (20 and 30 cm).

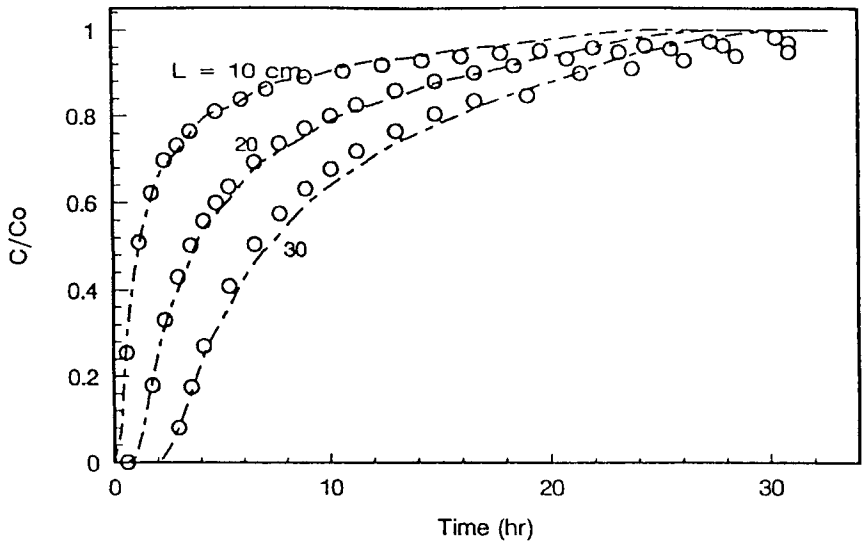

FIG. 6 Breakthrough curves for benzoic acid with the pore diffusion model. Open circles, experimental data; dashed lines, fitting (10 cm) and prediction (20 and 30 cm).

earlier than the experiments when generated from the pore model (Fig. 6). The solid model seems to give better results than the pore model in cases of favorable adsorption isotherms, although both can essentially be said to be in good agreement with the experimental.

The extent of agreement by employing different diffusion models to simulate a fixed-bed adsorber can be attributed to the inherent features of the models. The adsorption process described by the solid-diffusion model can be expressed in the following sequence: 1) the solute moving in the mobile phase, 2) adsorption of the solute on the adsorbent's outer surface, and 3) solid diffusion of the solute into the interior of the adsorbent. On the other hand, the adsorption process based on the pore-diffusion model can be stated as: 1) the solute moving in the mobile phase, 2) pore diffusion of the solute into the adsorbent, and 3) adsorption of the solute on the inner surface of the adsorbent. As pictured by the solid-diffusion model, the adsorption step begins only at the outer surface of the adsorbents. According to the pore-diffusion model, however, the solute can diffuse into the pore, and adsorption mainly occurs on the internal surface area of the adsorbents. Besides the availability of adsorption area, the magnitude of intraparticle diffusivity should also be taken into account. As indicated above, the effective pore diffusivity D_e is two orders of magnitude larger than the solid diffusivity D_s. The combined effect of a larger adsorption area and a faster intraparticle diffusion rate suggests that the pore model will predict a breakthrough curve which reaches the saturation point earlier than the solid model.

The very favorable adsorption isotherm for the solid-diffusion model can be attributed to the rate of adsorption (including ion-exchange reaction). In the case of a very rapid adsorption rate, there will be little pore diffusion involved because solute molecules have little chance to diffuse into the adsorbent particles in the unadsorbed state. In addition to the shape of the adsorption isotherm, the suitability of various diffusion models should at least also depend on two other factors: type of adsorbent and handling of equilibrium data. In the present cases, both factors favor the choice of the solid-diffusion model. First, ion-exchange materials are not considered porous unless they are inorganic and/or mineral, or have an usual resin structure interlaced with true internal pores due to a separate step in the synthesis (13). Accordingly, the amount of solute accumulated in the pore volume, which appears when employing the pore model, results in an underestimation in the effluent concentration. Second, in the handling of equilibrium data, q was measured by

$$q = \frac{(C_i - C_e)V}{W} \tag{20}$$

Equation (20), although widely used in both models, is essentially based on the solid-diffusion model. According to the pore-diffusion model, the exact expression of q should be

$$q = \frac{(C_i - C_e)V - C_e V_p}{W} \tag{27}$$

It can be seen that only if the total pore volume V_p is very small compared to the liquid volume V can the error introduced by employing Eq. (20) in the pore-diffusion model be ignored.

The computation time required to obtain a breakthrough curve depends on the number of collocation points and the steepness of the adsorption isotherm, as shown in Table 1. The computation times for benzoic acid were larger than those for *o*-cresol when using the same diffusion model. This result is not surprising because the shape of the adsorption isotherm of benzoic acid is steeper than that of *o*-cresol (see Figs. 1 and 2). In the case of benzoic acid, it can be seen that less computation time was required for the solid model than for the pore model. The computation times for the solid-diffusion model varied from 6 to 33 seconds when the number of collocation points varied from 5 to 8; the computation times for the pore-diffusion model varied from 11 to 74 seconds under the same range of number of collocation points. In the case of *o*-cresol, the computation times for both models varied from 4 to 27 seconds, with a smaller effect for the diffusion model. The accuracy of the model computation depends on the number of collocation points used. In this study, five collocation points in both column length and particle radius were sufficient for *o*-cresol with both the solid and pore models and for benzoic acid with the solid model. However, up to seven collocation points were needed for

TABLE 1
Comparison of Computation Times[a] for Different Models and Number of Collocation Points to Calculate a Breakthrough Curve

Collocation points[b]	Computation times (seconds)			
	Benzoic acid		*o*-Cresol	
	Solid	Pore	Solid	Pore
5	6	11	4	4
6	12	22	10	7
7	19	40	15	12
8	33	74	27	21

[a] Done on a 486 personal computer.
[b] In both column length and particle radius.

benzoic acid with the pore model to obtain satisfactory results. From the point of view of computation time, therefore, the solid-diffusion model is more effective in the time-domain parameter estimation than the pore-diffusion model, especially for steep adsorption isotherms.

The solid diffusivity D_s has been reported to be concentration-dependent. This can be anticipated because the property of an ion-exchange resin may change after the solute molecules have been adsorbed. Sudo et al. (14) pointed out that D_s can be correlated against q_0 by

$$D_s = D_{s0} \exp(aq_0) \tag{28}$$

Thus, a plot of ln D_s versus q_0 will give a straight line of slope a. D_{s0}, the solid diffusivity at zero coverage, is determined from the D_s value extrapolated to $q_0 = 0$. Equation (28) is in accordance with the data obtained in this study, as shown in Fig. 7. The point that the solid diffusivity D_s is a function of solute concentration is important for a successful simulation of a fixed-bed adsorber.

CONCLUSIONS

Intraparticle diffusion is an important mass transfer step in an adsorption process. Both solid- and pore-diffusion models have been widely used to describe diffusion in a porous adsorbent. In fitting an experimental

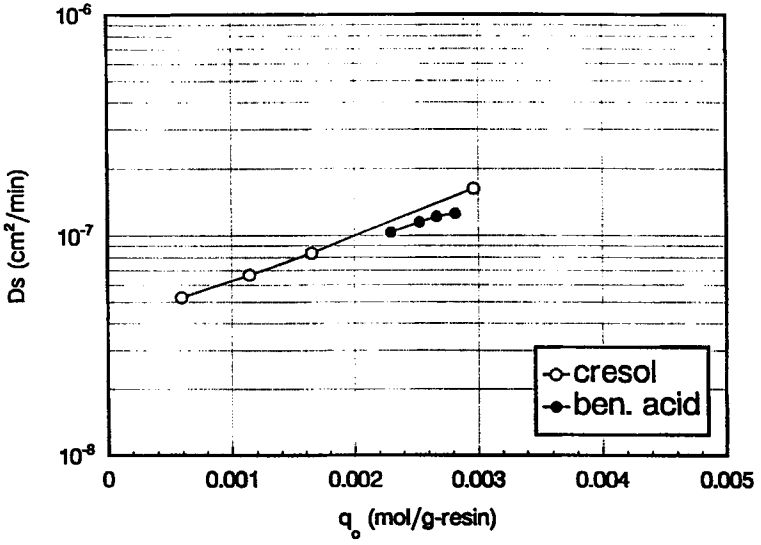

FIG. 7 Concentration dependence of solid diffusivity D_s.

breakthrough curve, these two models can be successfully employed to simulate various types of adsorption isotherms (linear, favorable and unfavorable isotherm shapes). Accordingly, it is not practical to judge the suitability of different diffusion models for the prediction of breakthrough curves without further empirical examinations. In the present study, experiments of the adsorptions of *o*-cresol and benzoic acid on fixed-bed columns of various lengths packed with an anion-exchange resin were performed. Equilibrium data showed an approximately linear adsorption isotherm for *o*-cresol and a favorable one for benzoic acid. An alternative form of the Langmuir adsorption isotherm (Eq. 26) was found to be adequate for modeling the equilibrium data. Better results in scale-up studies were found with the solid-diffusion model than with the pore-diffusion model if the shape of the adsorption isotherm was to be favorable. The factors that should be considered for successful simulations include the shape of the adsorption isotherm, the type of adsorbent, modeling of equilibrium data, computation efficiency, and concentration dependence of the intraparticle diffusivity.

ACKNOWLEDGMENT

This study was partly supported by Research Grant NSC83-0402-E006-09, National Science Council of the Republic of China.

NOMENCLATURE

a	constant in Eq. (28) (g-resin/mol)
C	solute concentration in mobile phase (mol/cm^3)
C_e	solute concentration in liquid phase at equilibrium (mol/cm^3)
C_i	initial solute concentration used in the equilibrium experiment (mol/cm^3)
C_p	solute concentration in pore (mol/cm^3)
C_s	fluid phase concentration near the particle surface (mol/cm^3)
C_0	inlet concentration of solute (mol/cm^3)
D_e	effective diffusivity for pore diffusion (cm^2/min)
D_L	axial dispersion coefficient (cm^2/min)
D_m	molecular diffusivity (cm^2/min)
D_s	surface diffusivity (cm^2/min)
D_{s0}	surface diffusivity at zero coverage defined by Eq. (28) (cm^2/min)
K	Langmuir constant defined by Eq. (24) (cm^3/mol)
k_f	film mass transfer coefficient (cm/min)
L	bed length (cm)
q	solute concentration in solid phase (mol/g-resin)

q_m maximum solid phase concentration of solute (mol/g-resin)
q_0 solid phase concentration of solute in equilibrium with C_0 (mol/g-resin)
R particle radius (cm)
r radial distance from center of spherical particle (cm)
Re Reynolds number ($2Ru_0\rho_L/\mu$) (dimensionless)
Sc Schmidt number ($\mu/\rho_L D_m$) (dimensionless)
t time (minutes)
u_0 superficial velocity (cm/min)
V liquid volume (cm^3)
V_p total pore volume (cm^3)
v interstitial fluid velocity (cm/min)
W weight of resin (g)
z distance in flow direction (cm)

Greek Letters

α coefficient in Langmuir isotherm defined by Eq. (4) or Eq. (13) (dimensionless)
ϵ_b bed void fraction (dimensionless)
ϵ_p intraparticle void fraction (dimensionless)
μ liquid viscosity (g/cm·min)
ρ density of the adsorbent particle (g-resin/cm^3)
ρ_L density of liquid (g/cm^3)

REFERENCES

1. J. B. Rosen, *J. Chem. Phys.*, *20*, 387 (1952).
2. T. W. Weber and R. K. Chakravorti, *AIChE J.*, *20*, 228 (1974).
3. A. Rasmuson and I. Neretnieks, *Ibid.*, *26*, 686 (1980).
4. T. L. Chen and J. T. Hsu, *Ibid.*, *33*, 1387 (1987).
5. C. Yao and C. Tien, *Chem. Eng. Sci.*, *47*, 465 (1992).
6. W. B. Bolden and F. R. Groves, *AIChE Symp. Ser.*, *264*(84), 62 (1987).
7. Mitsubishi Chemical Industries Limited, *Diaion: Manual of Ion Exchange Resins (I)*, revised ed., Tokyo, Japan, 1980, p. 89.
8. S. F. Chung and C. Y. Wen, *AIChE J.*, *14*, 857 (1968).
9. N. Wakao, T. Oshima, and S. Yagi, *Chem. Eng. Jpn.*, *22*, 780 (1958).
10. S. C. Foo and R. G. Rice, *AIChE J.*, *21*, 1149 (1975).
11. C. R. Wilke and P. Chang, *Ibid.*, *1*, 264 (1955).
12. G. S. G. Beveridge and R. S. Schechter, *Optimization: Theory and Practice*, McGraw-Hill, New York, 1970, p. 189.
13. R. H. Perry and C. H. Chilton, *Chemical Engineers' Handbook*, 5th ed., McGraw-Hill, New York, 1973, p. 16-4.
14. Y. Sudo, D. M. Misic, and M. Suzuki, *Chem. Eng. Sci.*, *33*, 1287 (1978).

Received by editor August 16, 1993